CHAPTER VII

A HEURISTIC FOR 3D FRICTIONAL FORCE CLOSURE GRASP

In this chapter, we pursue the same approach as in the case of 3D frictionless grasp discussed in the previous chapter. We present a heuristic for 3D four finger frictional force closure grasp and its use as a filtering criteria.

7.1 Introduction

A 3D frictional grasp is significantly distinct from the previous three categories of grasp, namely, the 2D frictionless grasp, the 2D frictional grasp and the 3D frictionless grasp, because a contact wrench set can not be represented by a polyhedral convex cone. This nonlinearity was a major roadblock for grasp analysis and synthesis problem because no sophisticated method was derived to solve this nonlinear problem. A traditional workaround is to linearize a friction cone by an m-sided pyramid which resulted in a finite number of primitive contact wrenches for each contact. This approach inevitably sacrifices some accuracy.

It is the work of Han, Trinkle and Li (2000) that tackles this nonlinearity problem directly. The work, based on the research of Buss, Hashimoto and Moore (1996), formulates the friction constraints as linear matrix inequalities (LMIs) and transforms the problem into a convex optimization problem. This method is complete, i.e., it considers directly the quadratic friction cone without linearization. However, it comes with the cost of efficiency since convex optimization takes considerable amount of computation power.

In this chapter, we study the problem of force closure testing with the motivation to improve computational efficiency while still maintaining the accuracy from the nonlinear model of friction cones. In particular, the main contribution of the chapter is a new necessary condition of force closure. The condition, geometrically derived from the nonlinear friction model, can be computed very efficiently.

In our experiments in which large number of grasps on various objects are tested, the performance improvement by using our method as a filtering criteria compared with using a complete test alone is paramount. In some cases, speed-up factor of 20 or greater can be achieved. The performance advantage is indeed desirable to the search based scheme in which many queries need to be made. To the best of our knowledge, this filtering approach to force closure testing with

nonlinear friction cones has never been presented before in the literature.

The rest of the chapter is organized as follows. In Section 7.2, we describe the main condition of our method which consider positively spanning of force and torque space. The test of force space and torque space are described in Section 7.3 and Section 7.4, respectively. In Section 7.5 we present numerical examples comparing efficiency gained by our approach. Finally, Section 7.6 concludes our work.

7.2 Necessary Condition for Four Finger Force Closure Grasp

Similar to the frictionless case, we use Lemma 6.1 as our necessary condition. The heuristic considers the force subspace and the torque subspace of the wrenches. Since four contact points are considered, four choices of the origin are included in the heuristic.

In summary, our condition consists of five tests: one considers the force space and the other four consider the torque space. When any test fails, it is guaranteed that the tested grasp does not achieve force closure. Let the contact point be located at $\boldsymbol{p}_1, \ldots, \boldsymbol{p}_4$ and let F_i and $\mathcal{T}_i$ be the set of forces and the set of torques associated with the contact point at $\boldsymbol{p}_i$, Our five tests are listed as follows.

1. $F_1, \ldots, F_4$ must positively span the force space.
2. Let the origin be located at $\boldsymbol{p}_1$; $\mathcal{T}_2, \mathcal{T}_3, \mathcal{T}_4$ must positively span the torque space.
3. Let the origin be located at $\boldsymbol{p}_2$; $\mathcal{T}_1, \mathcal{T}_3, \mathcal{T}_4$ must positively span the torque space.
4. Let the origin be located at $\boldsymbol{p}_3$; $\mathcal{T}_1, \mathcal{T}_2, \mathcal{T}_4$ must positively span the torque space.
5. Let the origin be located at $\boldsymbol{p}_4$; $\mathcal{T}_1, \mathcal{T}_2, \mathcal{T}_3$ must positively span the torque space.

Section 7.3 and Section 7.4 describe the method to test whether the force space and the torque space are positively spanned.

7.3 $\mathbb{R}^3$-Positive Span of Force Components

This section introduces a method to test whether four 3D friction cones positively span $\mathbb{R}^3$. Since positively spanning property concerns only directions of vectors, it is sufficient to represent a cone by its axis, which is the inward normal vector of the contact point, and its half angle.

Let us denote by $\boldsymbol{n}_i$ and μ the unit inward normal of contact point $\boldsymbol{p}_i$ and the respective friction coefficient. The half angle of the friction cone of $\boldsymbol{p}_i$ is $\theta = \tan(\mu)$. In other words,

$F_i = \{\boldsymbol{f} | (\boldsymbol{f} \cdot \boldsymbol{n}_i)/|\boldsymbol{f}| \geq \cos\theta\}$. We also define a negative cone $-F_i = \{-\boldsymbol{f} | \boldsymbol{f} \in F_i\}$ to be the cone consisting of the negative of all members of F_i. The following lemma describes a necessary and sufficient condition for several force cones to positively span $\mathbb{R}^3$. The condition is essentially an extension of Proposition 2.9.

Lemma 7.1 *Let $F_1, \ldots, F_n$ be force cones of contact points at $\boldsymbol{p}_1, \ldots, \boldsymbol{p}_n$. These force cones positively span $\mathbb{R}^3$ if and only if there exists an intersection between the interior of the negative of any cone and the interior of the positive span of the other three cones.*

Proof: Let $\mathcal{W} = \text{SPAN}^+(\bigcup_{i=2}^{n} F_i)$. Assume that $\text{INT}(-F_1) \cap \text{INT}(\mathcal{W})$ is not empty. Let $\boldsymbol{v}$ be an arbitrary vector in the intersection. Since $\boldsymbol{v}$ is a member of the interior of $\mathcal{W}$, we can always find three non-coplanar vectors $\boldsymbol{w}_1, \boldsymbol{w}_2, \boldsymbol{w}_3$ in $\mathcal{W}$ such that $\boldsymbol{v}$ lies in the interior of the pyramid formed by these three vectors. Since $\boldsymbol{v}$ is the negative of $-\boldsymbol{v}$ which is a vector in F_1, Proposition 2.9 can be applied to deduce that $\boldsymbol{w}_1, \boldsymbol{w}_2, \boldsymbol{w}_3$ and $\boldsymbol{v}$ positively span $\mathbb{R}^3$. The condition is therefore sufficient.

To prove that the condition is necessary, we will show that if $\text{INT}(-F_1) \cap \text{INT}(\mathcal{W}) = \emptyset$, no vector in $-\mathcal{W}$ can be written as a positive combination of members of $F_1, \ldots, F_n$ (therefore they do not positively span $\mathbb{R}^3$). Let us assume oppositely that some vector in $-\mathcal{W}$ can be written as a positive combination of a vector $\boldsymbol{a} \in F_1$ and some vector in $\mathcal{W}$. Since $\text{INT}(-F_1) \cap \text{INT}(\mathcal{W}) = \emptyset$, $-\boldsymbol{a}$ does not lie in $\mathcal{W}$. This implies that there exists a bounding plane P of $\mathcal{W}$ such that $-\boldsymbol{a}$ is on the negative side of P. In other words, $\boldsymbol{a}$ lies on the positive side of P. Obviously, any vector in $-\mathcal{W}$ is on the negative side of P. Hence, it is not possible to write any vector in $-\mathcal{W}$ as a positive combination of $\boldsymbol{a}$ and some vector in $\mathcal{W}$. A contradiction results which indicates that the condition is necessary. ■

To test whether four friction cones positively span $\mathbb{R}^3$, we pick two arbitrary cones, says F_1 and F_2, and then check whether these two cones positively span $\mathbb{R}^3$. If they do not, we pick another cone, says F_3. From Lemma 7.1, the only possibility that these three cones positively span $\mathbb{R}^3$ is that $\text{INT}(-F_3) \cap \text{SPAN}^+(F_1 \cup F_2) \neq \emptyset$. Thus, we check for such intersection. If none such intersection exists, we take the last cone (F_4) into account. Again, by Lemma 7.1, we know that these four cones positively span $\mathbb{R}^3$ only when $\text{INT}(-F_4) \cap \text{SPAN}^+(F_1 \cup F_2 \cup F_3) \neq \emptyset$. The method to test whether a negative cone intersects with the positive span of one cone, two cones and three cones are described in Section 7.3.1, 7.3.2 and 7.3.3, respectively.

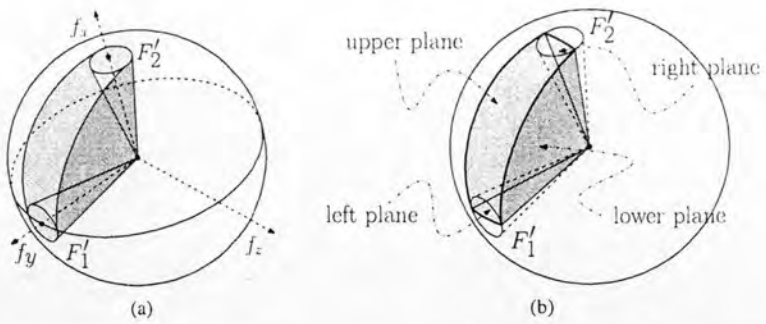

Figure 7.1: Two force cones and a unit sphere. (a) The shaded area represents the intersection between the positive span of two cones and the sphere. (b) The inner region containing the area $\text{SPAN}^+(F_1' \cup F_2')) - \text{INT}(F_2') - \text{INT}(F_2')$

7.3.1 Two Force Cones Positively Spanning $\mathbb{R}^3$

Let the two force cones be F_1 and F_2 (recall that these cones have their apex at the origin of the force space). From Lemma 7.1, two force cones positively span $\mathbb{R}^3$ only when there exists an intersection between the interior of one cone and the negative of the other cone. Two cones intersect when the angle between their axes is smaller than the sum of their half angles. Hence, to test whether F_1 and F_2 positively span $\mathbb{R}^3$, it is to be asserted whether the angle between $\boldsymbol{n}_1$ and $-\boldsymbol{n}_2$ is smaller than 2θ.

7.3.2 Three Force Cones Positively Spanning $\mathbb{R}^3$

Let the three force cones be $F_1, \ldots, F_3$. Let us assume that two of them, namely F_1 and F_2, do not positively span $\mathbb{R}^3$. From Lemma 7.1, to test if $F_1, \ldots, F_3$ positively span $\mathbb{R}^3$, it has to be asserted whether $\text{INT}(-F_3)$ intersects $\text{INT}(\text{SPAN}^+(F_1 \cup F_2))$. Observe that the condition is the same as asserting whether the vector $-\boldsymbol{n}_3$ intersects $\text{INT}(\text{SPAN}^+(F_1' \cup F_2'))$, where F_i' is the cone F_i whose half angle is increased by θ.

Since the condition concerns only the direction of force cones, let us represent a force cone by its intersection with a unit sphere. On the surface of the sphere, the intersection of $\text{SPAN}^+(F_1 \cup F_2)$ resembles a racetrack (see Figure 7.1a). Figure 7.2 displays the transformation.

When a vector $-\boldsymbol{n}_3$ intersects $\text{INT}(\text{SPAN}^+(F_1' \cup F_2'))$, it must lie in one of the following areas: 1) $\text{INT}(F_1')$, 2) $\text{INT}(F_2')$, and 3) the area in between F_1' and F_2'. The method tests whether $-\boldsymbol{n}_3$ lies in one of these areas. Each of the first two areas is simply a circular cone. The vector $-\boldsymbol{n}_3$ lies in the interior of a circular cone only when the angle between $-\boldsymbol{n}_3$ and the

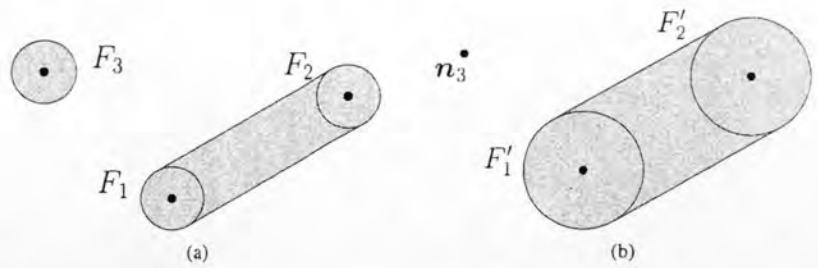

Figure 7.2: Force cones as seen on the surface of the unit sphere. The picture does not preserve linearity. (a) F_3 and $\text{SPAN}^+(F_1 \cup F_2)$. (b) Enlarging of F_1 and F_2 by θ.

axis of the cone is smaller than the cone's half angle. The in-between area is the remaining area $(\text{INT}(\text{SPAN}^+(F_1' \cup F_2')) - \text{INT}(F_1') - \text{INT}(F_2'))$. Instead of considering this area, we consider a four sided pyramid which is a super set of the in-between area and is a subset of $\text{INT}(\text{SPAN}^+(F_1' \cup F_2'))$. The pyramid, shown in Figure 7.1b, is bounded by four planes through the origin: two of which are the planes that are tangent to both F_1' and F_2' (see Figure 7.3a). We call these planes the upper and the lower planes. Each of the other two bounding planes is associated with each force cone. For each cone, we construct a bounding plane that contains the two tangent vectors at which the upper and the lower planes touch the cone. These two bounding planes are called the left plane and the right plane (also see Figure 7.3b).

Let P be the plane containing $\boldsymbol{n}_1$ and $\boldsymbol{n}_2$. Let $\boldsymbol{r}_i$ be the vector lying in P that is perpendicular to $\boldsymbol{n}_i$. We restrict $\boldsymbol{r}_1$ to point toward $\boldsymbol{n}_2$ and $\boldsymbol{r}_2$ to point toward $\boldsymbol{n}_1$, i.e., $\boldsymbol{r}_1 \cdot \boldsymbol{n}_2 > 0$ and $\boldsymbol{r}_2 \cdot \boldsymbol{n}_1 > 0$. Obviously, $\boldsymbol{r}_1$ and $\boldsymbol{r}_2$ are the normal vectors of the left and the right plane, respectively. The vectors on F_1' (resp. F_2') that are tangent to the upper and the lower planes can be calculated by rotating $\boldsymbol{n}_1$ (resp. $\boldsymbol{n}_2$) around $\boldsymbol{r}_1$ (resp. $\boldsymbol{r}_2$) by 2θ and -2θ. Figure 7.4 illustrates the calculation of the described normal vectors. With the normal vectors, testing whether $-\boldsymbol{n}_3$ lies inside the pyramid is simply testing the dot products between $-\boldsymbol{n}_3$ and the normal vectors.

7.3.3 Four Force Cones Positively Spanning $\mathbb{R}^3$

Let the four force cones be $F_1, \ldots, F_4$. Let us assume that three of them, namely F_1, F_2 and F_3, do not positively span $\mathbb{R}^3$. It has to be asserted whether $\text{INT}(-F_4)$ intersects $\text{INT}(\text{SPAN}^+(F_1 \cup F_2 \cup F_3))$. Analogous to the previous cases, it is to be asserted whether $-\boldsymbol{n}_4$ intersects $\mathcal{W}' = \text{INT}(\text{SPAN}^+(F_1' \cup F_2' \cup F_3'))$. Figure 7.5 illustrates $\mathcal{W}'$ as observed from the surface of the sphere. Obviously, $-\boldsymbol{n}_4$ is inside $\mathcal{W}'$ when either it is inside $\text{INT}(\text{SPAN}^+(F_1' \cup F_2'))$, inside $\text{INT}(\text{SPAN}^+(F_2' \cup F_3'))$, or inside $\text{INT}(\text{SPAN}^+(F_3' \cup F_1'))$, or, finally, inside the pyramid defined by the axes of the three cones. The last area is illustrated as the shaded region in Figure 7.5. The

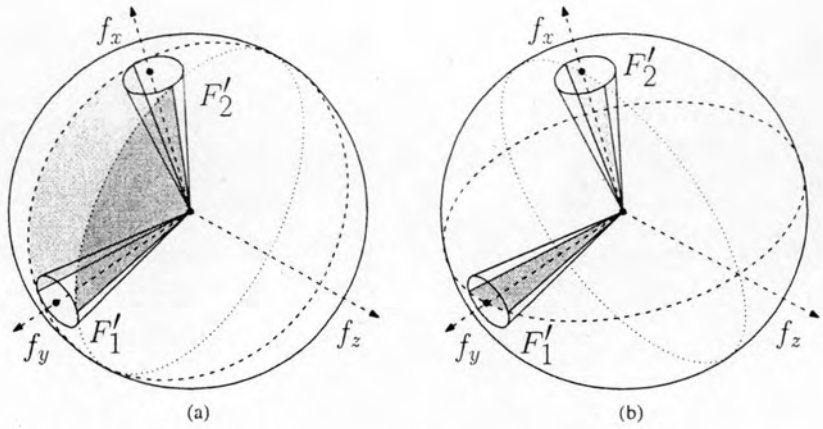

Figure 7.3: (a) The upper and lower plane, represented by the shaded area. The dashed line and the dotted line represent the great circles bounding the upper plane and the lower plane, respectively. The planes tangentially touch both cones. (b) The left and right plane, represented by the shaded area. The dashed line and the dotted line represent the great circles bounding the left plane and the right plane, respectively. The planes contain the double tangents of the same cone.

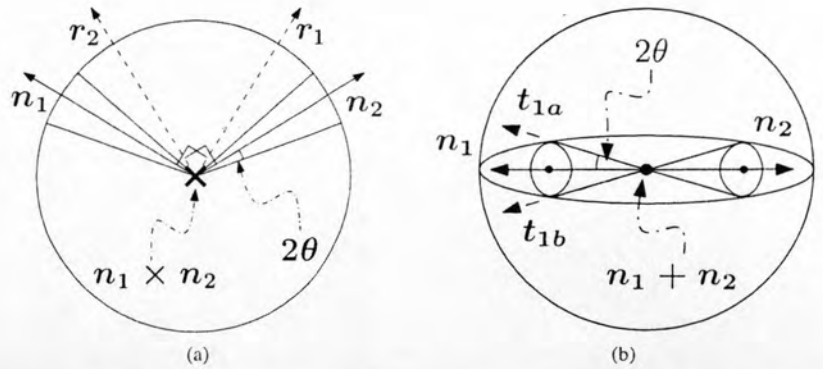

Figure 7.4: Computation of the planes bounding the pyramid. (a) The cone as viewed along $n_1 \times n_2$ which points into the page. The vectors r_1 and r_2 is the normal vector of the left and right plane. The vector n_1, n_2, r_1 and r_2 all lies on the same plane as the page. (b) The cones as viewed along $n_1 + n_2$ which points out from the page. The vector t_{1a} and t_{1b} are the double tangents of F_1' which is computed by rotating n_1 around r_1 by 2θ and -2θ, respectively.

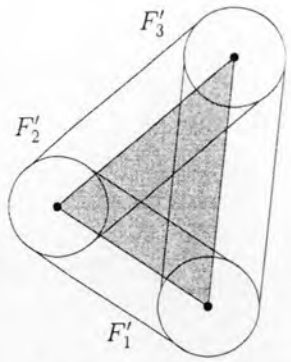

Figure 7.5: $\mathcal{W}'$ as seen on the surface of the sphere. The shaded region is the area need to be checked in addition to the other checking that can be done by the previous method.

method described in Section 7.3.2 can be employed to check the first three containments.

The intersection between $-\boldsymbol{n}_4$ and the pyramidal area can be tested by considering the dot products between $-\boldsymbol{n}_4$ and the inward normal vectors of the facets of the pyramid. The normal vectors of the three facets are ordered pairwise cross products of $\boldsymbol{n}_1$, $\boldsymbol{n}_2$ and $\boldsymbol{n}_3$. However, a correct order of $\boldsymbol{n}_1$, $\boldsymbol{n}_2$ and $\boldsymbol{n}_3$ has to be determined. There can be only two distinct orders, namely $(\boldsymbol{n}_1, \boldsymbol{n}_2, \boldsymbol{n}_3)$ or $(\boldsymbol{n}_2, \boldsymbol{n}_1, \boldsymbol{n}_3)$. The correct order can be obtained by considering the facet that contain $\boldsymbol{n}_1$ and $\boldsymbol{n}_2$. the normal vector of the facet that contain $\boldsymbol{n}_1$ and $\boldsymbol{n}_2$ is either 1) $\boldsymbol{n}_1 \times \boldsymbol{n}_2$ or 2) $\boldsymbol{n}_2 \times \boldsymbol{n}_1$. The correct direction is the one that has positive dot product with $\boldsymbol{n}_3$, because $\boldsymbol{n}_3$ must be on the positive side of the plane containing $\boldsymbol{n}_1$ and $\boldsymbol{n}_2$.

7.4 $\mathbb{R}^3$-Positive Span of Torque Components

This section examines the geometric relationship between the torque space and the friction cones. Let us denote by $\mathcal{T}_i$ the set of all torques generated by all forces in F_i (which is the friction cone of $\boldsymbol{p}_i$), i.e., $\mathcal{T}_i = \{\boldsymbol{p}_i \times \boldsymbol{f} | \boldsymbol{f} \in F_i\}$. Since any torque $\boldsymbol{p}_i \times \boldsymbol{f}$ is obviously perpendicular to $\boldsymbol{p}_i$, $\mathcal{T}_i$ must lie on the plane through the origin and perpendicular to $\boldsymbol{p}_i$. Let us call this plane P_i.

To describe how $\mathcal{T}_i$ occupies P_i, let us consider a plane P_f through the origin that contains $\boldsymbol{p}_i$ and intersects with F_i. Observe that a torque generated by any force in $P_f \cap F_i$ (a slice of F_i on P_f) must lie in the direction parallel to the normal of P_f. The idea is to consider all possible planes P_f so that all forces in F_i can be taken into account (see Figure 7.6a). With this idea, it can be shown that $\mathcal{T}_i$ lies on P_i in two different ways: 1) $\boldsymbol{p}_i$ is not in $\text{INT}(F_i)$. As the plane P_f rotates around $\boldsymbol{p}_i$ and continuously sweeps through F_i, correspondingly generated torques continuously sweep P_i. As a result, the resulting torques, $\mathcal{T}_i$, form a fan of torques, i.e., the set of all positive

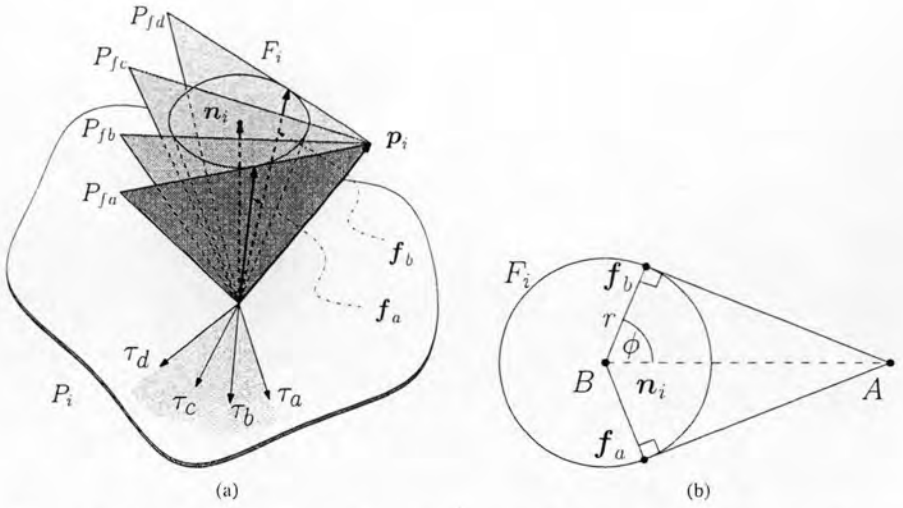

Figure 7.6: Torque plane. (a) A force cone F_i and its position vector $\boldsymbol{p}_i$. The curved line represents plane P_i which is perpendicular to $\boldsymbol{p}_i$. The plane $P_{fa}, \ldots, P_{fd}$ are planes through the origin that contains $\boldsymbol{p}_i$ and intersects F_i. P_{fa} and P_{fd} tangentially touch F_i and the intersection of which is $\boldsymbol{f}_a$ and $\boldsymbol{f}_b$, respectively. Vector $\tau_a, \ldots, \tau_d$ represents the direction of torque generated from $P_{fa}, \ldots, P_{fd}$, respectively. (b) The plane Π, lying perpendicular to $\boldsymbol{n}_f$ at the distance $\boldsymbol{p}_i \cdot \boldsymbol{n}_i$ from the origin. The radius of the boundary of the cone is $r = \tan(\theta)(\boldsymbol{p}_i \cdot \boldsymbol{n}_f)$. The angle ϕ equals to $\arccos(r/|\overline{AB}|)$.

combinations of two boundary torques. 2) When $\boldsymbol{p}_i$ is in $\text{INT}(F_i)$, $\mathcal{T}_i$ covers the entire plane P_i. This is the case because for each possible P_f, resulting torques span two opposite directions on P_i. Since P_f in this case can take any orientation around $\boldsymbol{p}_i$ to intersect with F_i, resulting torques cover all directions in P_i.

To compute the resulting fan of case 1, it is necessary to identify the two boundary torques of the fan. Since each of these torques is generated when P_f touches F_i, let us describe how to compute the corresponding forces $\boldsymbol{f}_a, \boldsymbol{f}_b \in F_i$ at which this event occurs. Let Π be the plane lying perpendicular to $\boldsymbol{n}_i$ at the distance $\boldsymbol{p}_i \cdot \boldsymbol{n}_i$ from the origin. Consider the intersection of Π with F_i and the lines through the vectors $\boldsymbol{n}_i, \boldsymbol{p}_i, \boldsymbol{f}_a, \boldsymbol{f}_b$. Figure 7.6b illustrates this intersection as observed on Π. From the figure, $\boldsymbol{f}_a$ and $\boldsymbol{f}_b$ can be determined from the angle ϕ. Let A and B be the intersection on Π of the line through $\boldsymbol{p}_i$ and the line through $\boldsymbol{n}_i$, respectively. The angle ϕ is equal to $\arccos(r/|\overline{AB}|)$ where r is the radius of the circle from the intersection of F and Π, i.e., $r = \tan(\theta)(\boldsymbol{p}_i \cdot \boldsymbol{n}_i)$.

7.4.1 Three Torque Sets Positively Spanning $\mathbb{R}^3$

We have established that a torque set of any contact point is either a fan or a plane. The problem is to assert whether three torque sets positively span $\mathbb{R}^3$. When any of the torque sets forms a plane, these sets positively span $\mathbb{R}^3$ only when there exists vectors lying on different sides

of this plane. Let $\boldsymbol{n}_t$ be the normal vector of the plane. If the other two sets are fans, we check whether the dot products between the boundary vectors of the fans and $\boldsymbol{n}_t$ have different signs. If the other sets are planes, we check whether the normal vectors of the other planes are not parallel to $\boldsymbol{n}_t$.

The remaining case is when all three torque sets are fans. It is equivalent to consider whether the six boundary wrenches of the fan positively span the plane. This problem is exactly the same as in the case of frictionless contact. The same method described in Section 6.4 is used in this case.

7.5 Numerical Comparison

The comparison in this chapter follows the same setting as in the case of frictionless grasp presented in Section 6.5. However, a different complete test method is used in this frictional case. We select a complete test for force closure presented by Han, Trinkle and Li (2000) for comparison. The method in (Han et al., 2000) is selected because it considers directly the quadratic friction cone without linearization, yielding most theoretical accuracy.

7.5.1 Method for Force Closure Test by Han et al.

Briefly speaking, the method in (Han et al., 2000), formulate the problem as an *LMI feasibility problem*. A grasping configuration is described by a vector $\boldsymbol{x} = \{x_{11}, x_{12}, \ldots, x_{ij}, \ldots, x_{nm}\}$ and a mapping matrix G. The component x_{ij} of vector $\boldsymbol{x} \in \mathbb{R}^{mn}$ indicates the magnitude of j^{th} component of intensity vector at i^{th} contact point and n, m indicates the number of contact point and the number of components of intensity vectors. In the case of a hard contact with friction, the intensity vector is the force vector which has three components. The matrix $G \in \mathbb{R}^{6 \times mn}$ transforms $\boldsymbol{x}$ into a wrench. The resulting wrench is equal to $G\boldsymbol{x}$. A nontrivial solution to $G\boldsymbol{x} = 0$ indicates an equilibrium grasp. We let V be a matrix whose columns are basis vectors of the null space of G. Hence, an equilibrium grasp can be written as $\boldsymbol{x} = V\boldsymbol{z}$ where $\boldsymbol{z}$ is a free variable.

Based on the work of Buss et al. (1996), the Coulomb Friction model can be represented in the form of LMI as $P(\boldsymbol{x}) \succeq 0$ where $\succeq 0$ denotes semi-positive definiteness. When the inequality is written as positive definite condition, i.e., $P(\boldsymbol{x}) \succ 0$, the force is restricted to lies in the interior of the friction cone. Since non-marginal equilibrium implies force closure, force closure test can

Table 7.1: Result of the Experiment

Objects	Time (seconds)		Speedup Factor	#Solution	#FP	Specificity
	Unfiltered	Filtered				
(a)	15,486.24	709.62	21.82	253,420	110,093	0.972
(b)	15,027.49	264.77	56.76	66,654	38,357	0.990
(c)	15,207.18	248.24	61.26	42,366	32,450	0.991
(d)	14,969.37	269.55	55.53	193,242	39,279	0.990
(e)	14,024.22	513.66	27.30	203,994	115,685	0.970
(f)	11,825.03	1,041.63	11.35	916,434	635,014	0.871
Avg.	14,423.26	507.91	39.01	279,352	161,813	0.964

be asserted from whether $P(Vz) \succ 0$ has an admissible solution. This inequalities can be solved by a traditional convex optimization technique.

7.5.2 Comparison and Result

The same set of objects in Figure 6.4 is used in this comparison. For each objects, $C_{100,4}$ grasps are generated. The friction coefficient is assumed to be $\tan(10°)$. Both methods are implemented in C++ using the convex optimization package *maxdet* (Wu et al., 1996) and the linear algebra package *LAPACK* (Anderson et al., 1999). The comparison is run on Pentium 4 3.0GHz with 1GB of memory. The result of the comparison is shown in Table 7.1. The second and the third column show the actual running time of the method in (Han et al., 2000) and the filtered version, respectively. Speedup factor is given in the forth column. The number of force closure grasps is given in the fifth column while the number of false positives of our condition is given in the sixth column. The seventh column gives the specificity of our test.

The result from the experiment shows similar results as in the case of 3D frictionless grasp. However, since the time used by the complete method in this case is significantly longer, the result is much more emphasized. The time used per query of our condition and of the method of Han et al. is approximately 0.0056ms and 3.6783ms, respectively. This indicates that, for each true negative solution, a running time is reduced to approximately 0.15%. In the case of false positive, the running time is increased to 100.15%. From the average specificity shown in Table 7.1, approximately 96.4% of the negative solutions is correctly identified by our condition. These figures indicate that the benefit of our condition is much more noticeable than the frictionless case.

The number of non force closure grasps varies significantly in the case of frictional grasp. For example, the circular object (f) has least number of non force closure grasps, i.e., least chance for the filtering criteria to express its benefit and thus the speed up in this case is minimum. On the

contrary, the complex object (c) has a large number of non force closure grasps and the speed up in this case is the greatest. Nevertheless, the filtered method using our condition takes one order of magnitude lower running time than the unfiltered version.

7.6 Summary

In this chapter we propose a necessary condition for force closure of a hard frictional contact points. The condition considers the quadratic friction cone without linearization. We also provide an implementation of the test based on the condition which utilizes the structure of force and torque of a hard contact. Specifically, we propose a simple method to assert whether four force cones positively span the force space. It also shows that the torque set associated to the force cone is either a fan or a plane. A method to test whether torque sets positively span the torque space is also introduced.

The benefit of the method is that it can be computed using relatively low computational effort. This allows the condition to be used as a filtering criteria which a grasp must be satisfied before a complete force closure assertion method is applied. From the numerical example. This approach could greatly speeds up the running time in the case of multiple force closure queries which proven to be useful in many situations.

Finally, we would like to discuss possible solution to force closure analysis. Let us consider the necessary condition used in our heuristic approach. The condition requires that several choices of origins are to be considered. This is because different origins give different torques. It can be seen that there might be underlying correlation between the number of origins used in the condition and the specificity of the test; a more number of origins yield a higher specificity of the test. It is tempting to generalize this observation to the extreme. For example, if all possible choices of the origin are made and all of them result in positively spanning in the torque space, one might conclude that the grasp achieve force closure. This is formalized in the following conjecture.

Conjecture 7.2 *A grasp achieve force closure when there is no origin such that the torques of the contact points, with respect to that origin, do not positively span the torque space.*

Interestingly, Reuleaux method is a kinematic counterpart of the above conjecture. If it is

known that this conjecture is true, force closure analysis could concentrate on torque component. This could be very beneficial because, in the case of 3D frictional grasp, the wrenches set associated with the contact points not linear, while the torque set is. Though it is still undetermined whether the problem is linear as a whole, it is worth to investigate this conjecture further.